Study of Ba₂Li₂Si₂O₇:Eu²⁺ phosphor for enhancing the luminous flux of white LEDs

Ha Thanh Tung[1], Huu Phuc Dang[2]
[1]Faculty of Basic Sciences, Vinh Long University of Technology Education, Vinh Long Province, Vietnam
[2]Faculty of Fundamental Science, Industrial University of Ho Chi Minh City, Ho Chi Minh City, Vietnam

Article Info

ABSTRACT

The best spectrum characteristics and photometric productivities of white light emitting diode (WLED) device possessing light emitting diodes (LEDs) in red rather than phosphor pc/R-WLEDs with the hue fidelity index (R_f) > 97 for correlated color temperatures (CCTs) between 2700 K and 6500 K were attained using the illumination effectiveness (LE) model. We demonstrate four practical pc/R-WLEDs that have indices of R_f and LE of 96–97 and 120–124 lm/W, respectively, under CCT values measured at 2969 K, 4468 K, 5682 K, as well as 6558 K. These LED packages use blue and red LEDs, also phosphors in green as well as yellow, with respective wavelengths of 448 nm, 650 nm, 507 nm, and 586 nm. In the comparison between phosphor-transformed WLED devices (with phosphor conversion) and quantum-dot WLED devices (QD-WLEDs), pc/R-WLEDs make an outstanding performance in competitiveness for high hue generation, particularly under small CCT values, and could eventually replace current pc-WLEDs.

Corresponding Author:

Huu Phuc Dang
Faculty of Fundamental Science, Industrial University of Ho Chi Minh City
Ho Chi Minh City, Vietnam
Email: danghuuphuc@iuh.edu.vn

1. INTRODUCTION

Phosphor-transformed white light emitting diode (WLED) device, quantum dots white light emitting diode (LEDs), and phosphor-coated white LED with red LEDs instead of phosphor (pc/R-WLED) are three different types of high-efficiency hybrid white LEDs. Color rendering properties that are near to the optimal or natural illumination supply, as well as outstanding performance, have long been desired. The overall hue rendering index (R_a) [1] and luminous efficacy (LE) [2] are commonly used to assess the effectiveness of hybrid white LEDs. In [3], [4], we investigated the optimum of white LEDs with the constraints of a predetermined correlated color temperatures (CCT) and R_a by increasing radiation luminous efficacy (LER). CCT adjustable and phosphor-converted WLED devices accompanied by an InGaN chip in blue, an AlGaInP chip in red, along with silicate phosphors in green as well as yellow under CCT values ranging from 2700 to 6500 K may produce LERs greater than 296 lm/W when R_a and R_9 were both greater than 98 [3]. At CCTs ranging from 2700 to 6500 K, quantum-dot WLED (QD WLED) devices including QDs in red, green as well as yellow, which were stimulated via a blue LED, exhibited LER values measured at 327–371 lm/W with R_a and R_9 values of 95 [4]. We developed the notion of limited luminous efficacy (LLE) to account for the energy loss induced by the Stokes shift [5]. Several improved mixing WLEDs were researched via enhancing LLE beneath specified hue rendering circumstances [5]-[9]. Phosphor-converted and CCT-adjustable WLEDs accompanied by phosphors in blue, red, green, as well as yellow may obtain values of LLE

measured at between 276 and 309 lm/W with R_a as well as R_9 over 98 under values of CCT ranging between 2700 and 6500 K [5].

The QD-WLED device will employ $CsPb(Cl_{0.1}Br_{0.9})_3$, $CsPb(Br_{0.9}I_{0.1})_3$ in green, $CsPb(Br_{0.5}I_{0.5})_3$ in yellow, and $CsPb(Br_{0.2}I_{0.8})_3$ in red. Under values of CCT ranging between 2700 K and 6500 K, three QDs operated via the chip in blue may achieve CCT adjustable illumination in white yielding R_aS measured at 96 to 97 along with LLE values measured at 243–254 lm/W [9]. The red-yellow-clear WLED device will produce CCT adjustable illuminations in white yielding R_aS value measured at 98 to 99, R_aS value measured at 98, as well as LLE values measured at 267 to 282 lm/W under values of CCTs measured at between 2700 K and 6500 K. Particularly, this WLED cluster includes AlGaInP LEDs in red under 633 nm, 20 nm, phosphor-converted yellow LEDs packed with phosphors in silicate green under 512 nm, along with orange under 580 nm, and InGaN colorant under 452.6 nm, 25.7 nm, along with phosphor-converted WLEDs using a silicate green phosphor under 512 nm and InGaN colorant. At CCTs ranging between 2731 K and 6533 K, the genuine red-yellow-white LED group will provide CCT adjustable white illumiations yielding R_aS values measured at 97 to 98, R_9S values measured at 98 to 99, along with values of LE measured at 122 to 132 lm/W [10]. R_a is a widely used color rendition metric. One issue with R_a is that it may award quite elevated ratings to supplies that depict saturated item hues extremely badly [11], [12]. The IES (short for Illuminating Engineering Society of North America) recently established one program that incorporates hue consistency indicator (R_f) as well as comparative hue scale indicator (R_g) for solving $R_a'S$ restrictions [13]. The approach has been accepted by the Commission Internationale de l'Eclairage (CIE) for advice from other countries [14].

Based on IES testing, the values of R_fS in phosphor-converted yellow WLED devices, QD WLED devices, along with the mentioned red-yellow-white LED group remained under 95, leading to the devices' hue generation characteristics being lower than R_a. Judging Yang *et al.*'s work [15], LEDs possessing four pathways yielding illumination in red, yellow, green, as well as blue along with blue LED devices will produce strong hue generation regards to R_f between 93 to 94 along with R_a between 95 to 97, as well as moderately good LER value between 299 and 339 lm/W throughout one broad CCT scope from 2800 K to 6500 K. They also presented a realistic seventeen-pathway LED setting including thirteen strait-line LED forms along with four phosphor-transformed WLED forms yielding R_fS value measured at 93 between 97, R_gS value between 100 and 102, as well as LER value between 282 and 312 lm/W under CCT values between 2800 and 6500 K. We could not find any information on how well the seventeen-pathway LED setting illuminated. The LLE, nonetheless, relies on the notion that photons received similar amount of photons emitted. Lately, an LE optimization model for CCT adjustable pc-WLEDs was developed [16]. At CCTs ranging from 2700 K to 6500 K, optimum phosphor-converted WLED devices containing phosphors in green, yellow, as well as red combined with one blue chip can obtain an R_f reaching 97, LE values between 118 and 127 lm/W towards radiance effectiveness (or R_e) for the blue-chip at 60% as well as quantum performance (Q_e) for the phosphor film at 90%.

Under CCT values measured at 3037 K, 4081 K, 4951 K, as well as 6443 K, multiple practical phosphor-converted WLEDs yielding R_fS values measured at between 96 and 97 as well as LE values measured at between 93 to 106 lm/W have been reported [17]. For the task of assessing the photometric productivitity for multiple mixing WLED forms, the LE design of pc/R-WLEDs must be established. Until now, studies have barely investigated the spectrum improvement for CCT adjustable phosphor-converted red WLED device via optimizing LE beneath certain value of R_f. This work suggests a design for the LE in phosphor-converted red WLED device, which included R_eS values in LED devices in red as well as red, along with Q_e for the double-hue film of phosphor. The adjusted spectrum characteristics in every hue element, along with the photometric as well as colorimetric productivities in phosphor-converted red WLED device utilized to optimize the mean LE under CCT values between 2700 K and 6500 beneath R_f 97, are given. In addition, the photometric productivities in mixing WLEDs yielding R_f value of 97 are studied by LE groups. At CCTs measured at 2969 K, 3955 K, 5034 K, as well as 6558 K, four of the most promising candidates were proven: phosphor-converted red WLED devices yielding R_f values measured at between 96 and 97 as well as LE values measured at between 120 and 124.

2. COMPUTATIONAL RECREATION
2.1. Creating $Ba_2Li_2Si_2O_7$:Eu^{2+}

The $Ba_2Li_2Si_2O_7$:Eu^{2+} composition is one of the essential parts of this study. Therefore, the substance must be well-prepared. Table 1 shows the combination of green $Ba_2Li_2Si_2O_7$:Eu^{2+} phosphor including 5 different ingredients. The phosphor can be obtained through combining, grinding, drying, powdering, along with 3 main heating steps. For the task of making a homogenous mixture, all of the

ingredients (except NH₄Br) must be dry milled or ground before beginning the first stage. Then, fire this combination in open quartz boats with H_2 at 850 °C for an hour; and now admit the NH₄Br by slurrying in methanol with a few cubic centimeters of water. Remove the mixture after 1 hour and dry it in the air. Next, powderize the dry mixture before putting it in capped quartz tubes for the second firing. This second-time heating phase lasts 1 hour and is carried out at 8500 °C, with N_2 flux. After this stage, the material will undergo another powdering process. After that, the last fire phase will be carried out in the same container and at the same temperature as the first, but with a CO solution and a 16-hour firing interval (leave overnight). After all, the outcome will be pulverized and stored in a well-sealed container. As a result, we can obtain the ideal blue-green-emitting $Ba_2Li_2Si_2O_7$:Eu^{2+} with the emitting highest point at 2.44 eV [18], [19]. The optical 3-D physical simulation and a real sample of WLED are shown in Figure 1.

Table 1. Constituents for $Ba_2Li_2Si_2O_7$:Eu^{2+}

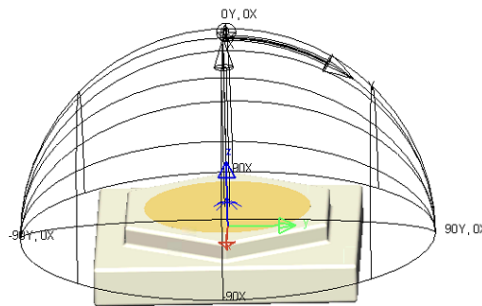| Ingredients	Mole %	By weight (g)
$BaCO_3$	97	191
Li_2CO_3	110 (of Li)	41
SiO_2	110	66
Eu_2O_3	3 (of Eu)	5.3
NH₄Br	50	49

Figure 1. Simulation of WLEDs

2.2. Photometric enhancement

The comparative spectrum energy dispensation (SPD) in phosphor-converted/red WLED ($S_{pc}/R(\lambda)$), which is composed of phosphor-coated LEDs (pc-LEDs) stimulated by blue and red LEDs, is given by the (1).

$$S_{pc/R}(\lambda) = k_{pc}S_{pc}(\lambda) + k_r S(\lambda, \lambda_r, \Delta\lambda_r) \tag{1}$$

$S_{pc}(\lambda)$ illustrates the comparative SPD in phosphor-converted LED, while $S(\lambda, \lambda r, \Delta\lambda r)$ illustrates the same aspect for LED in red, respectively. λ_r indicates the highest wavelength (WL). $\Delta\lambda_r$ indicates full breadth at half of the maximal value full width at half maximum (FWHM) of red LED. The terms k_{pc} and k_r indicate the spectra in phosphor-converted LED as well as LED in red, respectively. It is worth noting that the density factors (k_{pc} and k_r) only yield a separate index in the comparative SPD for phosphor-converted/red WLED. $S_{pc}(\lambda)$, the phosphor-converted comparative SPD, will be calculated (2).

$$S_{pc}(\lambda) = q_b S(\lambda, \lambda_b, \Delta\lambda_b + q_g S(\lambda, \lambda_g, \Delta\lambda_g) + q_y S(\lambda, \lambda_y, \Delta\lambda_y) \tag{2}$$

$S(\lambda, \lambda_b, \Delta\lambda_b)$ are the comparative SPD values for the blue spectrum transferred via the film of phosphor. In the case of $S(\lambda, \lambda_g, \Delta\lambda_g)$, and $S(\lambda, \lambda_y, \Delta\lambda_y)$, they indicate the transfer via phosphors in green and orange. The symbols λ_b, λ_g, and λ_y signify the highest wavelengths for blue LED, phosphors in green, and orange. $\Delta\lambda_b, \Delta\lambda_g$, and $\Delta\lambda_y$ represent their respective FWHMs. q_b, q_g, and q_y represent percentages for the comparative spectra for the spectrum in blue transferred by the film of phosphor, as well as green and orange phosphors. It's worth mentioning that the percentage coefficients, which are q_b, q_g, and q_y, in the comparative SPD from phosphor-converted LED only contain two independent components. In the case of LED devices in blue as well as red, we use the Ohno model [20] for SPDs. On the photon energy scale, phosphors' SPDs are described as a Gaussian function [21]-[23]. N_p is the quantity of low-power photons released per second by the green/yellow phosphor blend phosphor film.

$$N_p = \frac{k_{pc}q_g}{hc}\int_\lambda S(\lambda, \lambda_g, \Delta\lambda_g)\lambda d\lambda + \frac{k_{pc}q_y}{hc}\int_\lambda S(\lambda, \lambda_y, \Delta\lambda_y)\lambda d\lambda \tag{3}$$

The quantity of elevated-intensity photons in blue imbibed via the phosphor film in green or yellow each second is indicated by N_{ab}.

$$N_{ab} = \frac{q_{ab}}{hc}\int_\lambda S(\lambda, \lambda_b, \Delta\lambda_b)\lambda d\lambda \tag{4}$$

q_{ab}, h, and c denote the imbibed percentage for illumination in blue, the Planckian constant, and the speed of light, in turn. The assimilated fraction, q_{ab}, is assessed using the (5) since the green/yellow phosphor film's N_p/N_{ab} is specified as Q_e:

$$q_{ab} = \frac{k_{pc}q_g\int_\lambda S(\lambda, \lambda_g, \Delta\lambda_g)\lambda d\lambda + k_{pc}q_y\int_\lambda S(\lambda, \lambda_y, \Delta\lambda_y)\lambda d\lambda}{Q_e\int_\lambda S(\lambda, \lambda_b, \Delta\lambda_b)\lambda d\lambda} \tag{5}$$

The R_e of the blue LED is:

$$R_{e,b} = \frac{1}{P_{in,b}}\int_\lambda (k_{pc}q_b + q_{ab})S(\lambda, \lambda_b, \Delta\lambda_b)d\lambda \tag{6}$$

The R_e in the LED in red will be determined as:

$$R_{e,r} = \frac{1}{P_{in,r}}\int_\lambda k_r S(\lambda, \lambda_r, \Delta\lambda_r)d\lambda \tag{7}$$

$P_{in,b}$ and $P_{in,r}$ are the standardized supply energy in LED devices in blue as well red. As a result, the LE in phosphor-converted/red WLED, which includes the radiative effectiveness in LED devices in blue as well as red and the quantum effectiveness for the films of phosphor in green or yellow, is computed (8).

$$LE = \frac{683}{(P_{inb} + P_{inR})}\int_\lambda V(\lambda)S_{pc/R}(\lambda)d\lambda = \frac{\frac{683}{(P_{inb} + P_{inR})}\int_\lambda V(\lambda)S_{pc/R}(\lambda)d\lambda}{\frac{1}{R_{e,b}}\int_\lambda (k_{pc}q_b + q_{ab})S(\lambda, \lambda_b, \Delta\lambda_b)d\lambda + \frac{1}{R_{e,r}}\int_\lambda k_r S(\lambda, \lambda_r, \Delta\lambda_r)d\lambda} \tag{8}$$

$V(\lambda)$ represents the photopic illumination effectiveness function defined by the CIE in 1988. We propose the mean LE in CCT adjustable phosphor-converted/red WLED devices accompanied by blue as well as red LED components yielding values of $R_{e,b}$ and $R_{e,r}$ at 60%, also the film of phosphor in yellow or green yielding Q_e value at 90% beneath the constraint R_f at 97 in the form of aim parameter F:

$$F = \sum_{j=1}^8 LE_j (k_{r,j}, \lambda_b, \lambda_g, \lambda_y, \lambda_r, \Delta\lambda_g, \Delta\lambda_y, \Delta\lambda_r) \tag{9}$$

2700, 3000, 3500, 4000, 4500, 5000, 5700, and 6500 K of CCTs are represented by j = 1, 2, 3, 4, 5, 6, 7, and 8. The mixing WLEDs' hue was limited to be among the the Planckian position under CCT less than 5000 K, or the sun light position under CCT greater than 5000 K. As such, the hue distinction compared to the Planckian or sun light position judging the hue graph of CIE 1960 UV (D_{uv}) would reach 0. The purpose of the $D_{uv} = 0$ constraint is to prevent LED and phosphor peak WL and FWHM fluctuations from exceeding the hue deviation quadrangles for white-illumination supplies [19]-[20]. The chosen WLs for our pc/R WLED improvement range from 450 nm to 470 nm in the case of the LED in blue, 490 nm to 550 nm in the case of the phosphor in green, 550 nm to 600 nm in the case of the phosphor in yellow, as well as 600 nm to 650 nm in the case of the LED in red. Furthermore, the FWHMs of blue LEDs range from 25 to 35 nm, green and yellow phosphors from 70 to 120 nm, and red LEDs from 20 to 30 nm. The possible vectors are found on the hypersurface with 9 dimensions [24] when the twelve-dimension index zone is subjected to three hue-combining limitations, therefore the aim index F lacks the factors k_{pc}, q_b, q_g, as well as q_y. As a result, the optimizing issue is reduced to determining the optimum for F. For enhancement, the rapid Pareto genetic algorithm [25] would be used for its ability to find out various solving answers, without needing a beginning answer, would be ideal for intricate issues, along with the feature of fast alteration for approaching the Pareto optimum set.

With the LightTools 9.0 software along with Monte Carlo procedure, the study employed sheets of phosphor created via level films of silicone. The recreation method will be performed during certain stages, which include defining as well as building MCW-LED formation as well as its light properties. Thorough assessment is needed in order to gauge the influence from YAG:Ce^{3+} as well as Ba$_2$Li$_2$Si$_2$O$_7$:Eu^{2+} compounding that is imposed upon the performance for the device's lights. Two-sheet phosphor is considered having two blend forms having median CCT values reaching 3000 K, 4000 K, as well as 5000 K.

A description for MCW-LED lamps daubed in phosphor mixture as well as a median CCT value measured at 8500 K is displayed by Figure 1. The recreation for MCW-LED device lacking $Ba_2Li_2Si_2O_7:Eu^{2+}$ can be considered. The bottom length of the reflector is 8 mm, the height is 2.07 mm with the peak exterior length reaching 9.85 mm. We apply the conformal phosphor mixture to nine chips. All chips are 0.08-mm thick and linked with the reflector's gap by a square zone at 1.14 mm length, a height reaching 0.15 mm as well as one radiant flux measured at 1.16 watts accompanied by one highest wavelength measured at 453 nm.

3. RESULTS AND ANALYSIS

The correlation between $Ba_2Li_2Si_2O_7:Eu^{2+}$ and $YAG:Ce^{3+}$ is illustrated by Figure 2. The shift has two implications: it sustains median CCTs, affects absorptivity and dispersion for WLED devices containing dual films of phosphor, eventually altering the chroma along with the light beams' productivity efficiency in WLED devices. As such, the $Ba_2Li_2Si_2O_7:Eu^{2+}$ content will decide the color standard in the WLED device. The $YAG:Ce^{3+}$ concentration decreases as the $Ba_2Li_2Si_2O_7:Eu^{2+}$ concentration increases from 2% to 20% by weight in order to maintain the mean CCTs. WLEDs with CCT value range of 5600 K to 8500 K are no exception.
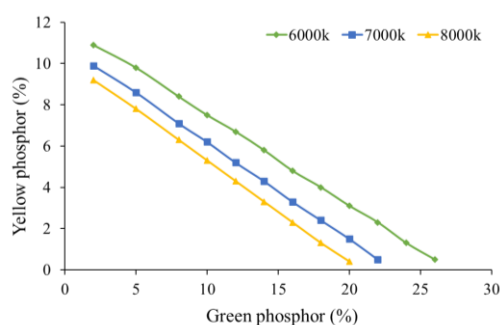
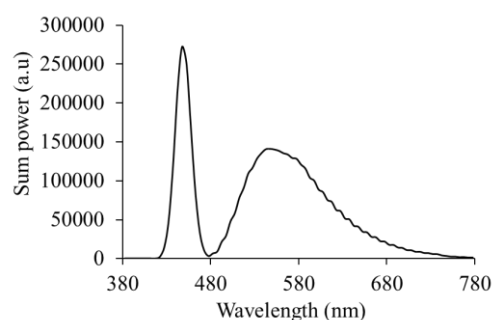Figure 2. Shifting the dosage for phosphor for keeping the median CCT

Figure 3. The correlation between the emitting spectra in 6000 K WLEDs and $Ba_2Li_2Si_2O_7:Eu^{2+}$ dosage

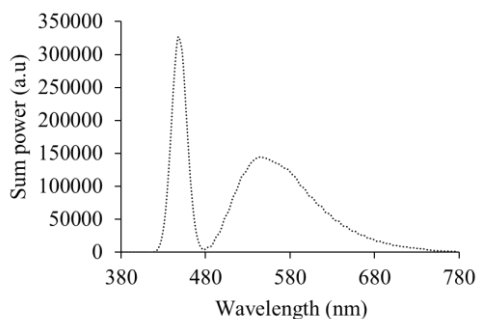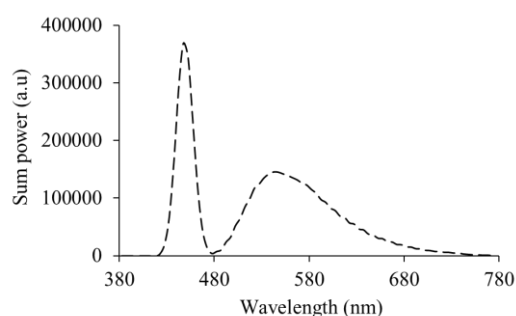Figure 4. The correlation between the emitting spectra in 7000 K WLEDs and $Ba_2Li_2Si_2O_7:Eu^{2+}$ dosage

Figure 5. The correlation between the emitting spectra in 8000 K WLED device and $Ba_2Li_2Si_2O_7:Eu^{2+}$ dosage

The transmission spectrum of WLEDs is influenced by the concentration of $Ba_2Li_2Si_2O_7:Eu^{2+}$ green phosphorus (Figure 3 to Figure 7). We may be able to come up with a selection according to the demands from the producer. WLEDs that demand excellent hue intensity can reduce the lighting beam by a little amount. The spectrum range merging illustrated by Figure 3 to Figure 7 is white light. These figures show spectra under 5600 K, 6600 K, 7000 K, 7700 K, along with 8500 K. In two parts of the light spectrum, the intensity trend increases with $Ba_2Li_2Si_2O_7:Eu^{2+}$ concentration: 420 nm – 480 nm along with 500 nm – 640 nm. Such growth of the double-line emitting spectra indicates a rise of the illuminating beam productivity. Furthermore, the blue-illumination dispersion from the WLED device is improved, implying that scatterings within the layer as well as the device are greater, favoring color homogeneity. This is an essential outcome when $Ba_2Li_2Si_2O_7:Eu^{2+}$ is utilzed. Managing the chromatic consistency for the phosphor arrangement at high temperatures, in particular, is difficult. These results proved that $Ba_2Li_2Si_2O_7:Eu^{2+}$, at hue heats of 5600 K along with 8500 K, may boost the hue intensity for the device.

Our study managed to gauge the performance of the generated illumination from the two-film phosphor setting. The results in Figure 6 show that the illuminance generated increases dramatically as the $Ba_2Li_2Si_2O_7:Eu^{2+}$ dosage raises 2% wt. 20% wt. According to Figure 7, the color divergence in all three means CCTs is greatly reduced when the phosphor $Ba_2Li_2Si_2O_7:Eu^{2+}$ concentration was increased. The outcome is a possible result of the red phosphor film's absorption. When the $Ba_2Li_2Si_2O_7:Eu^{2+}$ phosphor absorbs blue illumination generated by the chip in LED, the granules of blue phosphor change the illumination into green illumination. In addition to the blue illumination from the LED chip, the $Ba_2Li_2Si_2O_7:Eu^{2+}$ particles absorb yellow illumination. Nonetheless, when compared to these two absorbing features, the blue illumination absorption generated by said chip would be more potent owing to the material's absorbing features. By adding $Ba_2Li_2Si_2O_7:Eu^{2+}$, the green illumination from the WLED device increases, leading to an enhancement in the hue homogeneity index. Hue uniformity is an important property of current WLED lamps. Clearly, greater hue homogeneity would lead to greater WLED cost. The low cost of $Ba_2Li_2Si_2O_7:Eu^{2+}$ makes it an attractive option. Consequently, $Ba_2Li_2Si_2O_7:Eu^{2+}$ can be broadly used.

When evaluating the color standard of WLEDs, color consistency is merely one factor to consider. With a high color uniformity index only, a color standard cannot be said to be excellent. Later research presents chroma rendition index (CRI) as well as chroma quality scale (CQS). An entity reveals its actual color as it is brightly shone on. Superfluous green illumination among the main chromas of blue, yellow, as well as green causes color imbalance. The hue intensity of WLEDs is affected, leading to inferior WLED chroma fidelity. An insignificant CRI decrease is seen in Figure 8 when the $Ba_2Li_2Si_2O_7:Eu^{2+}$ film is added. Nevertheless, this minor penalty is permissible. As CRI is compared to CQS, CRI is inferior in assessment effectiveness owing to its small gamut for color reproduction. The CRI, the observer's desire, along with the chroma coordinate are indices included in the CQS assessment. In other words, CQS can be almost a true universal evaluation for choma standard for these three primary components. Figure 9 diaplays the CQS growth with a $Ba_2Li_2Si_2O_7:Eu^{2+}$ sheet's presence. Furthermore, regarding increasing $Ba_2Li_2Si_2O_7:Eu^{2+}$ content, CQS does not alter considerably as $Ba_2Li_2Si_2O_7:Eu^{2+}$ concentrations are below 10% wt. CRI and CQS would be considerably reduced when the $Ba_2Li_2Si_2O_7:Eu^{2+}$ concentration is greater than 10% wt., leading to significant waste of hue caused by green prevalence. Whenever $Ba_2Li_2Si_2O_7:Eu^{2+}$ is considered, appropriate dosage choosing is critical.
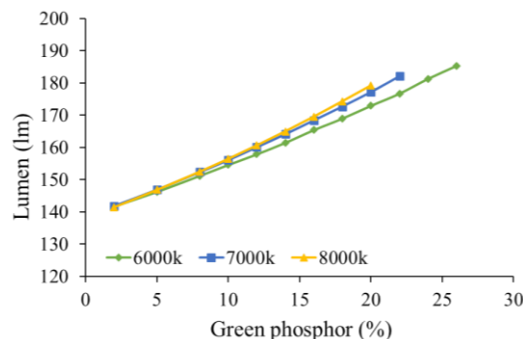

Figure 6. The correlation between the lumen in WLED device and $Ba_2Li_2Si_2O_7:Eu^{2+}$ dosage

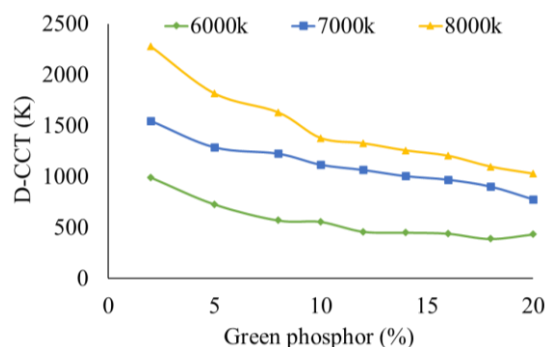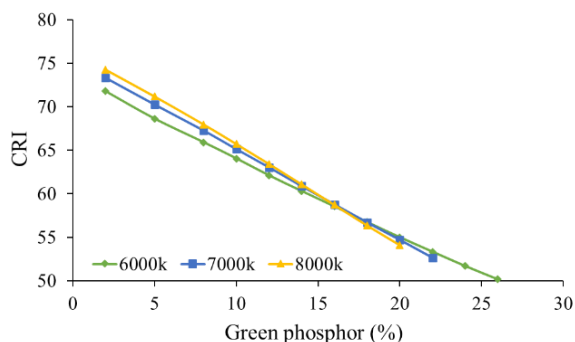Figure 7. The correlation between the hue aberration in WLED device and $Ba_2Li_2Si_2O_7:Eu^{2+}$ dosage

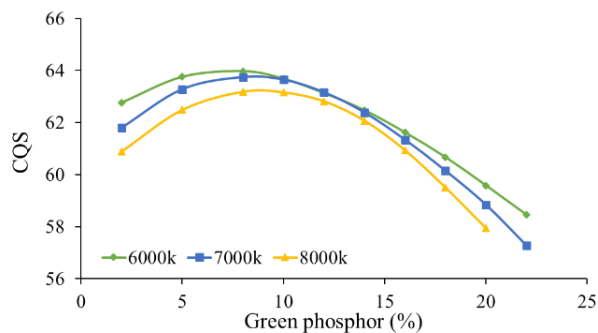Figure 8. The correlation between the CRI in WLED device and $Ba_2Li_2Si_2O_7:Eu^{2+}$ dosage

Figure 9. The correlation between the CQS in WLED device and $Ba_2Li_2Si_2O_7:Eu^{2+}$ dosage

4. CONCLUSION

The research depicts how $Ba_2Li_2Si_2O_7:Eu^{2+}$ would alter the optic features in the dual-sheet phosphor configuration. Using Monte Carlo computational models, the study displays that $Ba_2Li_2Si_2O_7:Eu^{2+}$ would be ideal at increasing hue homogeneity. This is true for WLEDs with a hue heat of more than 8500 K, as well as those with a low hue heat of 5600 K. As such, we managed to enhance the chroma standard as well as illumination beam, a difficult task for the phosphors' separate arrangement. Despite this, one minor flaw still exists in the case of CRI and CQS. The CRI, along with CQS, diminish substantially when the $Ba_2Li_2Si_2O_7:Eu^{2+}$ content becomes too high. Picking a proper content by considering the producers' objectives is vital. The article has provided a wealth of useful information as references to yield superior WLEDs' color homogeneity as well as intensity of light emissions.

REFERENCES

[1] V. -C. Su and C. -C. Gao, "Remote GaN metalens applied to white light-emitting diodes," *Optics Express*, vol. 28, no. 26, pp. 38883-38891, 2020, doi: 10.1364/OE.411525.

[2] F. -B. Chen, K. -L. Chi, W. -Y. Yen, J. -K. Sheu, M. -L. Lee, and J. -W. Shi, "Investigation on Modulation Speed of Photon-Recycling White Light-Emitting Diodes With Vertical-Conduction Structure," *in Journal of Lightwave Technology*, vol. 37, no. 4, pp. 1225-1230, 2019, doi: 10.1109/JLT.2018.2890331.

[3] S. Xu *et al.*, "Exploration of yellow-emitting phosphors for white LEDs from natural resources," *Applied Optics*, vol. 60, no. 16, pp. 4716-4722, 2021, doi: 10.1364/AO.424108.

[4] S. Keshri *et al.*, "Stacked volume holographic gratings for extending the operational wavelength range in LED and solar applications," *Applied Optics*, vol. 59, no. 8, pp. 2569-2579, 2020, doi: 10.1364/AO.383577.

[5] X. Xi, *et al.*, "Chip-level Ce:GdYAG ceramic phosphors with excellent chromaticity parameters for high-brightness white LED device," *Optics Express*, vol. 29, no. 8, pp. 11938-11946, 2021, doi: 10.1364/OE.416486.

[6] H. S. El-Ghoroury, Y. Nakajima, M. Yeh, E. Liang, C. -L. Chuang, and J. C. Chen, "Color temperature tunable white light based on monolithic color-tunable light emitting diodes," *Optics Express*, vol. 28, no. 2, pp. 1206-1215, 2020, doi: 10.1364/OE.375320.

[7] P. Zhu, H. Zhu, G. C. Adhikari, and S. Thapa, "Spectral optimization of white light from hybrid metal halide perovskites," *OSA Continuum*, vol. 2, no. 6, pp. 1880-1888, 2019, doi: 10.1364/OSAC.2.001880.

[8] Q. Xu, L. Meng, and X. Wang, "Nanocrystal-filled polymer for improving angular color uniformity of phosphor-converted white LEDs," *Applied Optics,* vol. 58, no. 27, pp. 7649-7654, 2019, doi: 10.1364/AO.58.007649.

[9] G. Zhang, K. Ding, G. He, and P. Zhong, "Spectral optimization of color temperature tunable white LEDs with red LEDs instead of phosphor for an excellent IES color fidelity index," *OSA Continuum*, vol. 2, no. 4, pp. 1056-1064, 2019, doi: 10.1364/OSAC.2.001056.

[10] B. Zhao, Q. Xu, and M. R. Luo, "Color difference evaluation for wide-color-gamut displays," *Journal of the Optical Society of America A*, vol. 37, no. 8, pp. 1257-1265, 2020, doi: 10.1364/JOSAA.394132.

[11] Q. Xu, B. Zhao, G. Cui, and M. R. Luo, "Testing uniform colour spaces using colour differences of a wide colour gamut," *Optics Express*, vol. 29, no. 5, pp. 7778-7793, 2021, doi: 10.1364/OE.413985.

[12] T. W. Kang *et al.*, "Enhancement of the optical properties of CsPbBr3 perovskite nanocrystals using three different solvents," *Optics Letters*, vol. 45, no. 18, pp. 4972-4975, 2020, doi: 10.1364/OL.401058.

[13] N. C. A. Rashid *et al.*, "Spectrophotometer with enhanced sensitivity for uric acid detection," *Chinese Optics Letters*, vol. 17, no. 8 2019, doi: 10.3788/COL201917.081701.

[14] P. Zhu, H. Zhu, G. C. Adhikari, and S. Thapa, "Design of circadian white light-emitting diodes with tunable color temperature and nearly perfect color rendition," *OSA Continuum*, vol. 2, no. 8, pp. 2413-2427, 2019, doi: 10.1364/OSAC.2.002413.

[15] L. Yang, Q. Zhang, F. Li, A. Xie, L. Mao, and J. Ma, "Thermally stable lead-free phosphor in glass enhancement performance of light emitting diodes application," *Applied Optics*, vol. 58, no. 15, pp. 4099-4104, 2019, doi: 10.1364/AO.58.004099.

[16] Y. Tian *et al.*, "Study of composite Al2O3-Ce:Y3Mg1.8Al1.4Si1.8O12 ceramic phosphors," *Optics Letters*, vol. 44, no. 19, pp. 4845-4848, 2019, doi: 10.1364/OL.44.004845.

[17] A. Ali *et al.,* "Blue-laser-diode–based high CRI lighting and high-speed visible light communication using narrowband green-/red-emitting composite phosphor film," *Applied Optics*, vol. 59, no. 17, pp. 5197-5204, 2020, doi: 10.1364/AO.392340.

[18] C. Wu, *et al.*, "Phosphor-converted laser-diode-based white lighting module with high luminous flux and color rendering index," *Optics Express*, vol. 28, no. 3, pp. 19085-19096, 2020, doi: 10.1364/OE.393310.

[19] R. Dang, H. Tan, N. Wang, G. Liu, F. Zhang, and X. Song, "Raman spectroscopy-based method for evaluating LED illumination-induced damage to pigments in high-light-sensitivity art," *Applied Optics*, vol. 59, no. 15, pp. 4599-4605, 2020, doi: 10.1364/AO.379398.

[20] S. Ma, P. Hanselaer, K. Teunissen, and K. A. G. Smet, "Effect of adapting field size on chromatic adaptation," *Optics Express*, vol. 28, no. 12, pp. 17266-17285, 2020, doi: 10.1364/OE.392844.

[21] D. Yan, S. Zhao, H. Wang, and Z. Zang, "Ultrapure and highly efficient green light emitting devices based on ligand-modified $CsPbBr_3$ quantum dots," *Photonics Research*, vol. 8, no. 7, pp. 1086-1092, 2020, doi: 10.1364/PRJ.391703.

[22] S. Feng and J. Wu, "Color lensless in-line holographic microscope with sunlight illumination for weakly-scattered amplitude objects," *OSA Continuum*, vol. 2, no. 1, pp. 9-16, 2019, doi: 10.1364/OSAC.2.000009.

[23] A. J. Henning, J. Williamson, H. Martin, and X. Jiang, "Improvements to dispersed reference interferometry: beyond the linear approximation," *Applied Optics*, vol. 58, no. 1, pp. 131-136, 2019, doi: 10.1364/AO.58.000131.

[24] R. Deeb, J. V. D. Weijer, D. Muselet, M. Hebert, and A. Tremeau, "Deep spectral reflectance and illuminant estimation from self-interreflections," *Journal of the Optical Society of America A*, vol. 36, no. 1, pp. 105-114, 2019, doi: 10.1364/JOSAA.36.000105.

[25] S. Kumar, M. Mahadevappa, and P. K. Dutta, "Extended light-source-based lensless microscopy using constrained and regularized reconstruction," *Applied Optics*, vol. 58, pp. 509-516, 2019, doi: 10.1364/AO.58.000509.

BIOGRAPHIES OF AUTHORS

Ha Thanh Tung received the PhD degree in physics from University of Science, Vietnam National University Ho Chi Minh City, Vietnam, he is working as a lecturer at the Faculty of Basic Sciences, Vinh Long University of Technology Education, Vietnam. His research interests focus on developing the patterned substrate with micro- and nano-scale to apply for physical and chemical devices such as solar cells, OLED, photoanode. He can be contacted at email: tunght@vlute.edu.vn.

Huu Phuc Dang received a Physics Ph.D degree from the University of Science, Ho Chi Minh City, in 2018. Currently, he is a lecturer at the Faculty of Fundamental Science, Industrial University of Ho Chi Minh City, Ho Chi Minh City, Vietnam. His research interests include simulation LEDs material, renewable energy. He can be contacted at email: danghuuphuc@iuh.edu.vn.